Re-evaluating the ^{238}U-salinity relationship in seawater: Implications for the ^{238}U–^{234}Th disequilibrium method

S.A. Owens [a,b,*], K.O. Buesseler [a], K.W.W. Sims [c]

[a] Department of Marine Chemistry and Geochemistry MS#25, Woods Hole Oceanographic Institution, 266 Woods Hole Road, Woods Hole, MA 02543, USA
[b] MIT-WHOI Joint Program in Oceanography/Applied Ocean Science Engineering, 266 Woods Hole Road, Woods Hole, MA 02543, USA
[c] Department of Geology and Geophysics, University of Wyoming, Dept. 3006, Laramie, WY 82071, USA

ABSTRACT

The concentration of ^{238}U in seawater is an important parameter required for applications of uranium decay-series radionuclides used to understand particle export and cycling in marine environments. Using modern mass spectrometer techniques, we re-evaluated the relationship between ^{238}U and salinity in the open ocean. The new ^{238}U-salinity relationship determined here is based on a larger sample set and a wider salinity range than previous work in the open ocean. Four samples from 500 to 1000 m in the subtropical Atlantic deviated significantly from their concentration predicted from salinity; these low concentrations are hypothesized to be the result of a remote removal process rather than analytical bias or local removal of uranium. We also bring attention to unique deficits of ^{234}Th in the mesopelagic zone of the subtropical Atlantic and encourage future applications of ^{234}Th to delve into the cause of these features. Determining the concentration of ^{238}U in the open ocean is critical for minimizing uncertainty in the ^{238}U-^{234}Th disequilibrium method, which is a key tool for understanding particle flux to the deep ocean.

© 2011 Elsevier B.V. All rights reserved.

1. Introduction

The marine geochemistry of uranium has been studied for several decades beginning with measurements of its speciation and distribution in the ocean (Ku et al., 1977) and expanding to studies of its daughter isotopes for tracers of past and present marine processes (Cochran, 1992). Measurements of uranium by alpha spectroscopy were some of the earliest to report conservative behavior of uranium with respect to salinity in the open ocean (Ku et al., 1977). A linear relationship between salinity and uranium concentration could only be established for the Antarctic and Arctic Oceans, due to the narrow range of salinities of the samples analyzed however. Later work used mass spectrometric techniques to perform similar measurements in the Atlantic and Pacific Oceans (Chen et al., 1986; Chen and Wasserburg, 1981). The relationship established by Chen et al. (1986) is still the most widely referenced value for determining uranium concentrations in seawater from salinity.

Despite the widespread use of the Chen et al. (1986) relationship, non-conservative behavior or deviations from this relationship have been reported in the open ocean. In a study of the Atlantic Ocean, it was hypothesized that low uranium-238 concentrations relative to salinity were due to the influence of Mediterranean Outflow Water (MOW) (Delanghe et al., 2002) but later work found no evidence to support this hypothesis (Schmidt, 2006). In another notable instance,

Robinson et al. (2004) measured higher values of ^{238}U in the Bahamas than predicted from salinity. In a review of ^{234}Th methodology, Rutgers van der Loeff et al. (2006) compiled ocean ^{238}U data and described possible causes of deviations from conservative behavior particularly sedimentary and estuarine addition and removal processes. Most recently, work in the Mediterranean Sea revealed higher ^{238}U concentrations than predicted from salinity (Pates and Muir, 2007). Pates & Muir (2007) hypothesized that deviation from the Chen et al. relationship may be significant in the Mediterranean Sea due to its large river inputs and its restricted exchange with the open ocean. They proposed a revised ^{238}U-salinity relationship, which combined previously published mass spectrometry data with their own, although they were not able to rule out analytical bias as a cause of variability between the studies. The resulting relationship between ^{238}U and salinity was not significantly different from that of Chen et al. however it resulted in a larger uncertainty than previously published (Pates and Muir, 2007).

The Chen et al. (1986) uranium-salinity relationship is frequently utilized in the ^{238}U-^{234}Th disequilibrium method, which is used to quantify particulate export flux and elucidate particle dynamics. This method takes advantage of the contrasting chemical behavior of uranium and thorium in seawater (Bacon et al., 1996; Bhat et al., 1969; Buesseler et al., 1992). At pH values and CO_2 concentrations typical of oxic seawater, the predominant uranium species, U(VI), is highly soluble and occurs as a stable carbonate ion complex, $UO_2(CO_3)_3^{4-}$ (Djogić et al., 1986). In contrast, Th(IV), the stable ion of thorium under oxic conditions, is highly particle reactive (Santschi et al., 2006). The 4.47×10^9 y half-life of ^{238}U

(Jaffey et al., 1971) greatly exceeds the 24.1 day half-life of its daughter, ^{234}Th. Due to the large difference in the half-lives of this parent–daughter nuclide pair, when there are no external forces adding or removing either of the two isotopes from the system, ^{238}U and ^{234}Th achieve a state of secular equilibrium after 5 to 6 half-lives of ^{234}Th. At secular equilibrium, the activity of ^{234}Th is equal to the activity of ^{238}U. In the surface ocean, a deficit of ^{234}Th activity (relative to ^{238}U) occurs when ^{234}Th sorbs to particulate matter and is removed as that material sinks. An excess of ^{234}Th can occur when dissolution or remineralization of sinking particles occurs, releasing ^{234}Th into solution deeper in the water column. This approach requires knowledge of the activity of both ^{234}Th and ^{238}U in seawater and the uranium-salinity relationship is a convenient means of estimating ^{238}U activity. Quantifying the uncertainty in the ^{238}U-salinity relationship can also be important for minimizing uncertainty in estimates of ^{234}Th flux. As illustrated in Fig. 6 of Pates & Muir (2007), a 1% difference in uncertainty of ^{238}U measurements can result in up to a 5% difference in ^{234}Th flux uncertainty.

Motivation for this work stemmed from observations of ^{234}Th during the Eddy Dynamic Mixing, Export, and Species (EDDIES) program in the Sargasso Sea, which studied the effect of eddy-induced changes on biogeochemical cycling (Buesseler et al., 2008a; McGillicuddy Jr. et al., 2007). Typically, deficits of ^{234}Th are constrained to the euphotic zone as a result of marine particle formation through primary production and subsequent removal by passive sinking of the particles (Bacon et al., 1996; Buesseler et al., 2008a, 2008b). In EDDIES however, at least three profiles of ^{234}Th were collected showing a ^{234}Th deficit relative to ^{238}U between 500 and 1000 m defined by at least three individual samples in each case. This ^{234}Th deficit tended to be co-located with the local oxygen minimum zone. This feature could be due to anomalous ^{238}U behavior at these depths or a particle repackaging process that was reflected in the ^{234}Th profile. Unfortunately, no samples for ^{238}U were collected during the EDDIES program. In other studies of ^{234}Th, similar features have been observed in one or two samples from intermediate depths however, because of its utility as a measure of export flux, most studies focus sampling efforts on the euphotic zone, providing limited depth resolution through the mesopelagic (Benitez-Nelson et al., 2001a; Coppola et al., 2005; Schmidt, 2006). In this work, we attempt to capture these unique ^{234}Th features with paired measurements of ^{238}U and ^{234}Th and increased sampling resolution through the mesopelagic zone to highlight unique and previously undescribed behavior of both ^{238}U and ^{234}Th at these depths. Finally we propose an alternate ^{238}U-salinity relationship developed from a large set of ^{238}U measurements that encompasses a wide range of salinity values and was obtained using sensitive mass spectrometric techniques.

2. Methods

2.1. Study sites

Samples were collected on three cruises to the Bermuda Atlantic Time-series Study site (BATS) on the R/V *Atlantic Explorer* in July 2007, June 2008, and September 2009, a cruise (SIRENA) across the tropical Atlantic on the R/V *Oceanus* in August 2009, and on three cruises to the Southern Ocean on the ARSV *Laurence M. Gould* in January 2009 and 2010 and on the RVIB *Nathaniel B. Palmer* in March 2010. Salinity values for the Southern Ocean samples were taken from CTD sensors, which were calibrated on an annual basis and exhibit an insignificant amount of drift between calibrations (e.g. $+0.00010$ psu month^{-1}). Salinity values for samples from the BATS site and the tropical Atlantic were made using a salinometer either on land or at sea.

2.2. ^{238}U Sampling and concentration measurements

Collection vials for ^{238}U were prepared by washing them in a 10% HCl solution followed by 5% HNO$_3$ solution, rinsing with ultra-clean water (18.2 MΩ) before and after each step. The vials were rinsed

with the sample water three times before filling and were then sealed with Parafilm® to prevent evaporation. Samples were stored in a dark, room-temperature environment until preparation for analysis.

^{238}U concentrations were determined by isotope dilution (ID) using a Thermo Scientific ELEMENT 2 Inductively Coupled Plasma Mass Spectrometer (ICP-MS). Teflon® vials were used throughout sample preparation and were subjected to rigorous cleaning including soaking and boiling in 50% HCl, soaking in aqua regia (1:3 HNO$_3$ and HCl), soaking and boiling in 50% HNO$_3$, and a final boil in weakly acidfed (HNO$_3$) water, with generous rinses of ultra-clean water between each step. Sample aliquots of 5 mL were spiked with a well-calibrated ^{233}U spike to achieve ^{238}U/^{233}U≈ 10; the collection vial, the spike bottle, and the Teflon vial into which the sample and spike were aliquoted, were weighed when sample or spike was removed or added in order to precisely determine the mass of sample and spike in each analysis aliquot. Samples were equilibrated and digested over the course of two days. First, samples were allowed to evaporate overnight at 75 °C in a laminar flow bench. After cooling, 1 mL concentrated HNO$_3$ was added to each sample, which was then capped and returned to the hot-plate for 15 min. Then 1 mL of Milli-Q water was added to each sample and samples were capped and left to sit overnight at room temperature to allow complete equilibration and digestion. Uranium was purified and separated from salts using anion exchange columns. Eichrom 2 mL acid-cleaned columns were prepared using 1 mL of pre-conditioned (50% HCl and dilute HNO$_3$ with Milli-Q rinses) Eichrom AG1$\times$8 anion exchange resin. Each column was further conditioned with Milli-Q, 10 M HCl, 1 M HCl, Milli-Q, and 7 M HNO$_3$. The dissolved samples (~7 M HNO$_3$) were loaded onto the columns and the sample dissolution vials were carefully rinsed with additional 7 M HNO$_3$. To collect uranium, the columns were eluted with Milli-Q, 1 M HCl, and 1 M HBr. Samples were dried overnight at a low temperature and then sample vials were stored in bags until analysis.

Immediately prior to analysis, samples were brought up in 1 mL of 5% HNO$_3$ and quickly measured in analog mode. Based on the initial intensity of the major isotope, ^{238}U, the samples were then diluted such that all isotopes of U were measured in ion counting mode. The instrument was tuned using the NBS-960 standard to achieve flat peak tops and stable signal intensity. Mass fractionation corrections were made by bracketing samples with the NBS-960 standard (^{238}U/^{235}U $= 137.88$) and using the linear average to correct the measured ^{238}U/^{235}U ($0.04 - 2.76\%$ correction) and ^{238}U/^{233}U ($0.07 - 4.55\%$ correction) ratios. Similarly, samples were blank corrected using bracketed blank acid samples. Background signals of ^{233}U and ^{238}U were less than 0.50% of the spike and sample signals. Prior to data collection, the in-growth of the NBS-960 or sample signal was observed until it appeared stable, at which point data collection was initiated. Each sample was analyzed in triplicate, so that each reported value is the average of these individual measurements. The propagated error includes the standard deviation of these three measurements, the uncertainty associated with weighing the sample and spike, and the uncertainty on the ^{233}U spike calibration. The measurement sequence for a single sample was: blank-NBS-960–blank–sample–sample–sample–blank–NBS960 and so forth. Samples of the International Association for Physical Sciences of the Ocean (IAPSO) Standard Seawater (OSIL P149) were analyzed to assess the reproducibility of the measurements over multiple runs on the ICP-MS and to establish a laboratory standard for future studies of ^{238}U in seawater. The calibration of our ^{233}U spike has also been verified in several studies using equilibrium rock standards (Sims et al., 2008).

2.3. ^{234}Th sampling and analysis

^{234}Th was determined using the 4 L method of co-precipitating ^{234}Th with MnO$_2$ and beta counting the samples on low background, coincidence detectors (Risø National Laboratories) either on land or at sea as soon as possible after collection (Benitez-Nelson et al., 2001b; Buesseler et al., 2001). Detector efficiency and background were determined at regular intervals over the period of this study. Final

sample counts, after five half-lives (>4 months), were performed to account for detector background and interfering beta emitters. Recovery efficiencies of the MnO_2 precipitation step were determined using a ^{230}Th yield monitor (Pike et al., 2005). The reported error on ^{234}Th values includes the counting error of the initial and final counts and the uncertainty of the percent recovery determination. In cases where multiple samples were collected at the same depth, the uncertainties of the ^{234}Th values are the standard deviation of these measurements.

3. Results

The samples analyzed for ^{238}U concentration in this study encompass a wider salinity range (32.688–37.102) than most other works that employ high precision mass spectrometric techniques (Fig. 1, Table 1). Andersen et al. (2007) is the only other study that has a wider salinity range (25.90–34.96, n = 20; see Table 2). The propagated error on the concentration measurements was 1.5%. To establish the reproducibility of our method, replicate analyses of IAPSO Standard Seawater and samples from the BATS site were made. Here a sample replicate is defined as a unique 5 mL aliquot from a single sample collection vial that has been equilibrated with ^{233}U, purified via column chemistry, and measured on the ICP-MS. IAPSO Standard Seawater (Salinity = 34.994) was measured nine times with an average ^{238}U concentration of 3.116 ± 0.028 ng g^{-1} and a relative standard deviation (RSD) of 0.9% (Tables 1 & 2). When two samples from the BATS site in June 2007 (100 and 800 m) were analyzed in triplicate, the resulting RSD of the three measurements was 1.2% and 0.6% respectively (Table 1). The RSD for all samples analyzed in this study (normalized to S = 35, without the four low BATS samples) is higher at 1.9% and may represent natural variability of ^{238}U concentration in the ocean relative to salinity (Table 2).

The linear relationship of ^{238}U with salinity in the open ocean provides a convenient way to estimate ^{238}U concentrations/activities without performing time-intensive analysis. Most of the samples analyzed in this study appear to vary linearly with salinity except for the four deepest samples from the BATS site in June 2007, which have lower ^{238}U concentrations than might be expected (Fig. 1a). These points are between 16 and 32% lower than predicted using the Chen et al. (1986) relationship. Possible explanations for these anomalously low values will be explored in the Discussion.

In prior studies of the relationship between ^{238}U and salinity, the standard procedure has been to normalize ^{238}U concentrations of samples to a salinity of 35 and take the average and standard deviation of the normalized values in order to establish a conversion factor from salinity to ^{238}U concentration/activity. The narrow salinity range of samples collected in a single study often precludes the determination of a robust linear relationship. By normalizing all the data, linearity or conservative behavior is inherently assumed, and the standard deviation is used to describe the goodness of fit. With this data set we were able to perform a linear regression (n = 87, excluding IAPSO samples and low concentration BATS samples) and determine an R^2 value for the fit. In units of ng g^{-1}, the equation for the best-fit line with an R^2 of 0.78 is:

$$^{238}U(\pm 0.061) = (0.100 \pm 0.006) \times S - (0.326 \pm 0.206). \qquad (1)$$

The root mean squared (rms) error for the regression is 0.061 (1σ); for a sample with a salinity (S) of 35, this results in a ^{238}U concentration of 3.174 ng g^{-1} with a 1.9% uncertainty.

For ^{234}Th/^{238}U disequilibrium studies however, the activity per unit volume (dpm L^{-1}) rather than the mass per unit mass (ng g^{-1}) is required. To convert from units of mass to activity we use Eq. (2):

$$^{238}U\left(dpm\ g^{-1}\right) = {}^{238}U\left(ng\ g^{-1}\right) \times 10^{-9} \times 1/m_a\left(^{238}U\right) \times N_A \qquad (2)$$
$$\times \ln(2) \times 1/t_{1/2}\left(^{238}U\right)$$
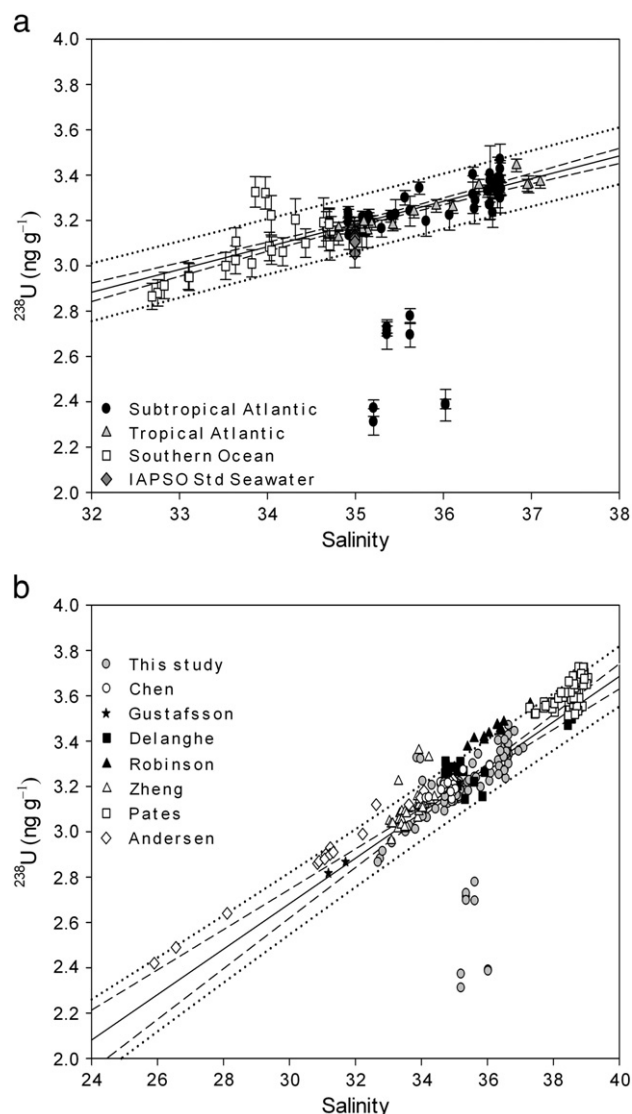
Fig. 1. Dissolved ^{238}U in seawater as a function of salinity. a) Results of mass spectrometry measurements of ^{238}U concentration in the subtropical and tropical Atlantic Ocean and the Southern Ocean. Also shown are measurements of IAPSO Standard Seawater used to confirm analysis reproducibility. The solid line is the best-fit line through all the data excluding the low subtropical Atlantic values and the IAPSO Standard Seawater analyses. The dashed lines denote the 95% confidence interval for the linear regression and the dotted lines denote the 95% prediction interval (the range within which future observations of ^{238}U vs. salinity should fall). Note that the anomalous Southern Ocean and subtropical Atlantic samples fall outside of the 95% prediction interval. b) Results from previous mass spectrometry studies of ^{238}U in the open ocean and from this work. Note the change in the scale for the x-axis. The lines are from the data in this study only (Fig. 1a), including the regression (solid), 95% confidence interval (dashed), and 95% prediction interval (dotted) lines.

where m_a is the atomic mass of ^{238}U (238.050783 amu), N_A is Avogadro's constant (6.022 × 10^{23} mol^{-1}), and the half-life of ^{238}U is 4.468 × 10^9 y (2.348 × 10^{15} min). The second conversion step that is required is from units per mass (g^{-1}) to units per volume (L^{-1}), which can be achieved by multiplying by the sample density (kg m^{-3}). The density of samples was calculated using the sample salinity and room temperature (20 °C, the temperature at which samples were aliquoted) with the SeaWater Library Version 1.2e released by CSIRO Marine Research, which uses the UNESCO equations of state (Millero and Poisson, 1981; UNESCO, 1983). A second linear regression

Table 1
[238]U concentration measurements by ICP-MS. Replicates are 5 mL aliquots from a single sample collection vial or Standard Seawater vial that have been prepared and analyzed individually.

Collection Location & Date	Depth (m)	Temperature (°C)	Salinity	O$_2$ (µmol kg^{-1})	[238]U (ng g^{-1})	± Error (ng g^{-1})
Subtropical Atlantic (BATS) 31.665°N×64.168°W	3.9[b]	27.390	36.620	205.4	3.373	0.028
July 18 2007	3.9[c]	27.390	36.620	205.4	3.387	0.092
	99.1[a]	19.140	36.646	211.7	3.426	0.028
	99.1[b]	19.140	36.646	211.7	3.469	0.068
	99.1[c]	19.140	36.646	211.7	3.386	0.078
	401.0[b]	17.730	36.531	212.2	3.375	0.028
	401.0[c]	17.730	36.531	212.2	3.405	0.124
	500.0[b]	16.800	36.337	194.7	3.402	0.033
	500.0[c]	16.800	36.337	194.7	3.314	0.083
	600.5[b]	15.010	36.026	177.9	2.390	0.021
	600.5[c]	15.010	36.026	177.9	2.385	0.070
	699.3[b]	12.450	35.622	162.0	2.778	0.033
	699.3[c]	12.450	35.622	162.0	2.695	0.054
	799.2[a]	10.160	35.359	156.3	2.712	0.022
	799.2[b]	10.160	35.359	156.3	2.728	0.025
	799.2[c]	10.160	35.359	156.3	2.697	0.065
	899.9[b]	8.280	35.206	169.7	2.372	0.036
	899.9[c]	8.280	35.206	169.7	2.311	0.058
Subtropical Atlantic (BATS) 31.765°N×64.311°W	25.6	22.953	36.616	227.0	3.320	0.064
June 27 2008	56.2	20.425	36.640	230.9	3.351	0.028
	75.1	19.745	36.649	229.5	3.343	0.028
	100.8	19.329	36.658	222.9	3.339	0.028
	126.0	18.757	36.615	212.7	3.328	0.027
	151.2	18.481	36.598	200.8	3.342	0.027
	176.2	18.306	36.582	199.7	3.342	0.031
	201.2	18.235	36.581	201.5	3.352	0.027
	300.6	17.691	36.505	203.3	3.329	0.027
	400.2	17.013	36.365	198.3	3.288	0.026
	600.3	13.382	35.729	171.2	3.342	0.027
	650.3	12.156	35.564	160.1	3.300	0.032
	700.4	10.848	35.402	154.5	3.219	0.026
	749.9	9.851	35.298	152.9	3.164	0.038
	800.9	8.642	35.186	157.9	3.189	0.032
	850.0	7.825	35.153	171.1	3.221	0.028
	901.0	7.218	35.153	186.2	3.208	0.026
	950.4	6.571	35.111	197.2	3.177	0.026
	1000.9	6.239	35.114	207.1	3.173	0.030
	1101.0	5.526	35.081	223.7	3.214	0.027
	3000.0	2.611	34.918	266.3	3.236	0.026
	3000.3	2.611	34.921	266.3	3.223	0.026
	3000.0	2.611	34.942	266.3	3.183	0.027
	3000.6	2.611	34.921	266.3	3.191	0.026
Subtropical Atlantic (BATS) ~31.467°N×~63.900°W	21.3	27.764	36.533	197.7	3.272	0.066
Sept 21–24 2010	175.7	19.345	36.646	200.0	3.299	0.066
	302.1	18.262	36.561	202.3	3.234	0.065
	402.9	17.928	36.524	197.2	3.269	0.066
	504.8	16.977	36.355	184.8	3.252	0.067
	606.0	15.376	36.070	169.9	3.223	0.066
	657.1	13.807	35.805	158.6	3.196	0.066
	706.1	12.611	35.621	150.0	3.241	0.066
	757.8	11.393	35.456	143.8	3.227	0.065
	906.7	7.852	35.129	167.1	3.145	0.065
	1008.7	6.376	35.072	200.2	3.148	0.066
	1518.0	4.299	34.987	250.4	3.134	0.081
	3043.4	2.766	34.928	267.3	3.134	0.063
Tropical Atlantic 13.071°N×40.628°W	58.4	24.909	36.969	196.0	3.359	0.037
Aug 15 2008	91.3	23.461	37.102	190.2	3.369	0.027
	100.0	22.181	36.954	182.8	3.355	0.027
	110.0	20.585	36.831	162.9	3.443	0.028
	150.4	17.643	36.405	121.7	3.355	0.027
	199.0	14.872	35.919	98.8	3.264	0.028
	250.4	13.370	35.666	90.4	3.238	0.027
	376.4	10.143	35.186	85.4	3.183	0.026
	439.7	9.233	35.059	93.8	3.167	0.033
Tropical Atlantic 11.715°N×28.861°W	5.8	28.535	36.106	196.9	3.258	0.026
Aug 24 2008	100.7	13.954	35.426	97.9	3.180	0.026
	200.6	11.592	35.139	114.5	3.154	0.025
	300.7	10.761	35.074	87.4	3.160	0.026
	439.3	9.998	35.096	48.4	3.193	0.026
	600.0	8.253	34.962	61.0	3.174	0.026

Table 1 (*continued*)

Collection Location & Date	Depth (m)	Temperature (°C)	Salinity	O$_2$ (µmol kg^{-1})	^{238}U (ng g^{-1})	± Error (ng g^{-1})
	850.0	6.163	34.811	104.0	3.166	0.026
	1001.8	5.473	34.809	131.3	3.125	0.033
Southern Ocean 68.252°S × 69.887°W	1.7	1.390	33.637	346.3	3.026	0.062
Jan 21 2009	18.4	1.070	33.641	363.3	3.106	0.062
	50.4	−0.003	33.862	352.1	3.326	0.068
	74.7	−0.520	33.977	333.1	3.321	0.071
	100.3	−0.540	34.174	283.2	3.062	0.062
	147.2	0.490	34.433	217.9	3.100	0.063
	296.2	1.430	34.671	178.6	3.175	0.064
Southern Ocean 68.394°S × 77.920°W	1.5	1.210	34.022	323.3	3.085	0.063
Jan 29 2009	40.1	0.460	34.043	349.9	3.223	0.087
	99.2	−0.120	34.318	235.6	3.205	0.091
	197.8	1.860	34.638	171.0	3.192	0.108
	396.2	1.880	34.705	177.1	3.129	0.063
	1283.5	1.190	34.723	195.2	3.155	0.063
	2557.8	0.560	34.704	207.8	3.191	0.064
	3165.4	0.420	34.701	211.8	3.185	0.064
Southern Ocean 69.501°S × 75.506°W	1.8	−1.250	32.752	381.2	2.880	0.058
Jan 27 2010	4.1	−1.370	32.688	377.0	2.865	0.058
	8.0	−1.250	32.827	386.7	2.913	0.058
	12.4	−0.650	33.100	406.1	2.955	0.059
	12.3	−0.670	33.111	349.4	2.950	0.059
	50.4	−1.170	33.524	322.0	2.999	0.060
	100.3	−1.540	33.822	291.7	3.010	0.060
	180.8	−0.950	34.047	258.9	3.067	0.061
Southern Ocean 70.420°S × 76.421°W	600.4	1.31	34.709		3.090	0.065
March 29 2010			34.994[d]		3.152	0.025
IAPSO Standard Seawater OSIL P149			34.994[d]		3.135	0.026
			34.994[d]		3.113	0.042
			34.994[d]		3.103	0.031
			34.994[c]		3.132	0.063
			34.994[e]		3.130	0.067
			34.994[e]		3.121	0.063
			34.994[f]		3.054	0.062
			34.994[f]		3.105	0.064

[a-f] Analysis dates of replicates of BATS samples and IAPSO standard seawater were: [a] Dec 21 2007, [b] Sept 2 2008, [c] May 11 2009, [d] Dec 17 2008, [e] Sept 27 2010, and [f] Oct 10 2010.

was performed on the data now in units of dpm L^{-1} and is expressed in Eq. (3).

$$^{238}U(\pm 0.047) = (0.0786 \pm 0.00446) \times S - (0.315 \pm 0.158) \qquad (3)$$

At S = 35, this results in a ^{238}U activity of 2.436 dpm L^{-1} with a 1.9% (1σ) uncertainty.

The linear regression of the data from this study (without the low concentration BATS samples) yields a y-intercept of −0.326 ± 0.206 ng g^{-1} or −1.369 ± 0.865 nmol kg^{-1} at zero salinity. The negative intercept implies a loss of uranium between its riverine source and the open ocean, however there is a large uncertainty on this y-intercept. From the oceanic uranium budget, we expect a uranium source, rather than sink, from rivers, which globally have a discharge, weighted mean concentration of 1.2 ± 0.3 nmol kg^{-1} (Dunk et al., 2002). Submarine groundwater discharge may also account for up to 20% of uranium input to the oceans, although this value is poorly constrained (Osmond and Cowart, 1992). Both sources and sinks of uranium in fresh water/seawater mixing zones have been noted (Andersen et al., 2007; Carroll and Moore, 1994; Dunk et al., 2002; Feng et al., 2002; McKee et al., 1987) and given the large uncertainty here on the y-intercept, it is difficult to resolve the global average impact of these processes. We suggest that the uranium-salinity relationship presented here should only be applied within the salinity range of ~32.7 to 37.1 and may not hold in lower salinity environments such as estuaries.

4. Discussion

This work set out to re-evaluate the conservative relationship between salinity and ^{238}U in the open ocean using sensitive mass spectrometric techniques. We have derived a new relationship for ^{238}U and salinity over a wider salinity range and with a larger number of samples than any previous single study (Fig. 1a). While most of the samples analyzed were conservative with salinity, deviations from this behavior were observed in a small number of samples. In the Southern Ocean, two samples lie just above the 95% prediction line for ^{238}U, while in the subtropical Atlantic, anomalously low concentrations of ^{238}U were observed between 500 and 1000 m. These anomalies within this single data set are discussed below but first we compare our results to previous studies to look at the overall trend of ^{238}U vs. salinity.

In Table 2, the salinity-normalized (S = 35) average concentration for our data set is compared to previous studies that used alpha spectroscopy or mass spectrometry. Within error, the average for this study is comparable to the averages from previous studies that employed either analytical technique. Similarly, the RSD of all the samples is within the range of those from previous mass spectrometry studies. More informative perhaps is to compare ^{238}U data obtained using the more precise mass spectrometric methods vs. salinity to see if there is a similar trend and anomalies in this relationship as we have found (Fig. 1b). While most measurements from previous studies fall within the 95% prediction interval of this study, some of the samples do fall outside, including Zheng et al. (2006) which lie near to some of

Table 2

A comparison of this work to previous studies. Results for alpha spectroscopy and mass spectrometry studies are shown separately. Results for this study were obtained as ng g^{-1} but have been converted to dpm/L (in italics) for comparison to alpha spectroscopy studies. Values in bold are the averages of all the data from each study. For the Atlantic and overall average values from this study, low values from BATS July 2007 are not included. (Andersen et al., 2007; Chen et al., 1986; Delanghe et al., 2002; Gustafsson et al., 1998; Ku et al., 1977; Pates and Muir, 2007; Rengarajan et al., 2003; Robinson et al., 2004; Schmidt, 2006; Schmidt and Reyss, 1991; Zheng et al., 2006).

|		Salinity range	N =	^{238}U concentrations normalized to salinity = 35					
				Average (dpm L^{-1})	Std. dev.	RSD %	Average (ng g^{-1})	Std. dev.	RSD %
Alpha spectroscopy studies									
Ku	Atlantic	34.459–36.140	28	2.48	0.08	3.1			
	Pacific	34.590–35.173	7	2.50	0.09	3.8			
	Arctic	30.300–34.940	13	2.54	0.03	1.1			
	Southern Ocean	33.492–34.732	19	2.43	0.04	1.6			
	All	**30.300–36.140**	**67**	**2.48**	**0.07**	**2.9**			
Schmidt & Reyss	Atlantic	35.61–36.45	7	2.57	0.07	2.7			
	Mediterranean	38.14–39.18	18	2.59	0.08	3.1			
	All	**35.61–39.18**	**25**	**2.58**	**0.08**	**3.1**			
Rengarajan	**Arabian**	**34.892–36.557**	**61**	**2.38**	**0.08**	**3.3**			
Schmidt	Atlantic	35.21–36.46	11	2.56	0.06	2.2			
	Mediterranean	35.98–38.43	2	2.64	0.10	3.6			
	All	**35.21–38.43**	**13**	**2.57**	**0.06**	**2.5**			
Pates & Muir	**Mediterranean**	**36.423–38.633**	**73**	**2.50**	**0.13**	**5.0**			
Mass spectrometry studies									
Chen	Atlantic	34.611–36.080	10				3.189	0.028	0.9
	Pacific	34.140–35.275	11				3.238	0.011	0.4
	All	**34.140–36.080**	**21**				**3.215**	**0.032**	**1.0**
Gustafsson	**Atlantic**	**31.18–31.70**	**2**				**3.164**	**0.003**	**0.1**
Delanghe	Atlantic	38.44–38.56	8				3.191	0.071	2.2
	Mediterranean	34.94–35.92	5				3.202	0.037	1.2
	Indian	34.72–35.28	8				3.283	0.039	1.2
	All	**34.72–38.56**	**21**				**3.229**	**0.067**	**2.1**
Robinson	**Atlantic**	**35.400–37.280**	**12**				**3.334**	**0.013**	**0.4**
Zheng	**Pacific**	**33.034–34.393**	**40**				**3.221**	**0.064**	**2.0**
Pates & Muir	**Mediterranean**	**37.278–39.055**	**68**				**3.268**	**0.045**	**1.4**
Andersen	**Arctic**	**25.90–34.96**	**20**				**3.25**	**0.03**	**0.9**
This study	Atlantic	34.809–37.102	63	*2.44*	*0.03*	*1.4*	3.187	0.044	1.4
	Southern Ocean	32.688–34.723	24	*2.44*	*0.07*	*3.0*	3.187	0.095	3.0
	IAPSO	34.994	9	*2.38*	*0.02*	*0.9*	3.117	0.028	0.9
	All	**32.688–37.102**	**87**	***2.44***	***0.05***	***2.0***	**3.187**	**0.062**	**1.9**

our high measurements from the Southern Ocean. Also, the samples from Robinson et al. (2004) all fall along the upper limit of our prediction interval, suggesting a possible bias (or local ^{238}U source) in their data set. A linear regression of the combined data ($n = 271$) has a strong R^2 of 0.92 (in ng g^{-1}, ^{238}U (± 0.065) = $(0.099 \pm 0.002) \times S - (0.238 \pm 0.063)$), but we cannot account for analytical bias and uncertainty in other studies so it is difficult to say if these anomalies are real. We focus our discussion on our own samples where the same methods and standards were used throughout.

We observed a slight elevation in ^{238}U in at least two samples collected in the Southern Ocean, a region where ice melt dynamics could potentially create unique distributions of ^{238}U. Ku et al. (1977) is the only study to present results of salinity and alpha-spectroscopy ^{238}U measurements from the Southern Ocean. The salinity normalized average ^{238}U activity measured by Ku et al. of 2.43 dpm L^{-1} is comparable to the value of 2.44 dpm L^{-1} reported here (Table 2). In recent work carried out at the ice-edge in the Weddell Sea, Rodriguez y Baena et al. (2008) measured the ^{238}U concentration of 26 samples and reported an average relative percent deviation of $1.9 \pm 2.3\%$ from the value published by Pates and Muir (2007) but generally conservative behavior overall. Unfortunately, paired salinity and uranium measurements were not provided in the publication for direct comparison to this work. Our Southern Ocean samples have a large scatter about the mean compared to Atlantic Ocean samples (Table 2) and in particular, samples from the first (50 and 75 m on Jan 21 2009) and second (40 and 100 m on Jan 29 2009) stations deviate from the values predicted by the linear regression by 3–8% (Fig. 1a). On a T-S plot these four samples did not appear to be part of a unique and distinct water mass that may have suggested a common source of

this increased variability such as melt waters, thus we cannot attribute this variability to differences in water mass properties.

The anomalous low ^{238}U concentration values measured at the BATS site in 2007 are the most obvious feature of this data set (Table 1, Fig. 1a). There are three possible explanations for this anomalous feature: (1) collection or measurement error, (2) local removal or (3) removal on the continental shelf/slope and subsequent advection to the study region. In regard to the first hypothesis, it seems unlikely that the low ^{238}U concentrations are a sampling artifact as all samples were collected in a uniform fashion and there is no apparent difference in the 2007 samples. Also, the entire 2007 profile was analyzed in duplicate or triplicate (Table 1, Fig. 2) with good reproducibility. Thus, the low values were not the result of differences in spike equilibration and sample purification or anomalous mass spectrometer behavior on a single day.

The second possibility, that the low uranium signal was generated as the result of a local process, causing uranium to be reduced and removed from the water column, seems unlikely. Firstly, oxygen concentrations in 2008 and 2009 when subsequent samples were collected were the same or lower than in 2007 and no low ^{238}U feature was observed in either year (Fig. 2). Secondly, samples measured at much lower oxygen concentrations in the subtropical Atlantic showed no deviation from salinity-derived values (Table 1). Even in a study of uranium cycling in the Black Sea, an anoxic basin with a long deep-water residence time, there was no evidence of uranium reduction in the water column (Anderson et al., 1989). Uranium occurred as U(VI) throughout the Black Sea even though it was shown to be labile and reducible by a strong reducing agent. The work of Anderson et al. (1989) supported previous results that suggested that at seawater U(VI) concentrations, an initial adsorption step onto clay particles is required for reduction to occur
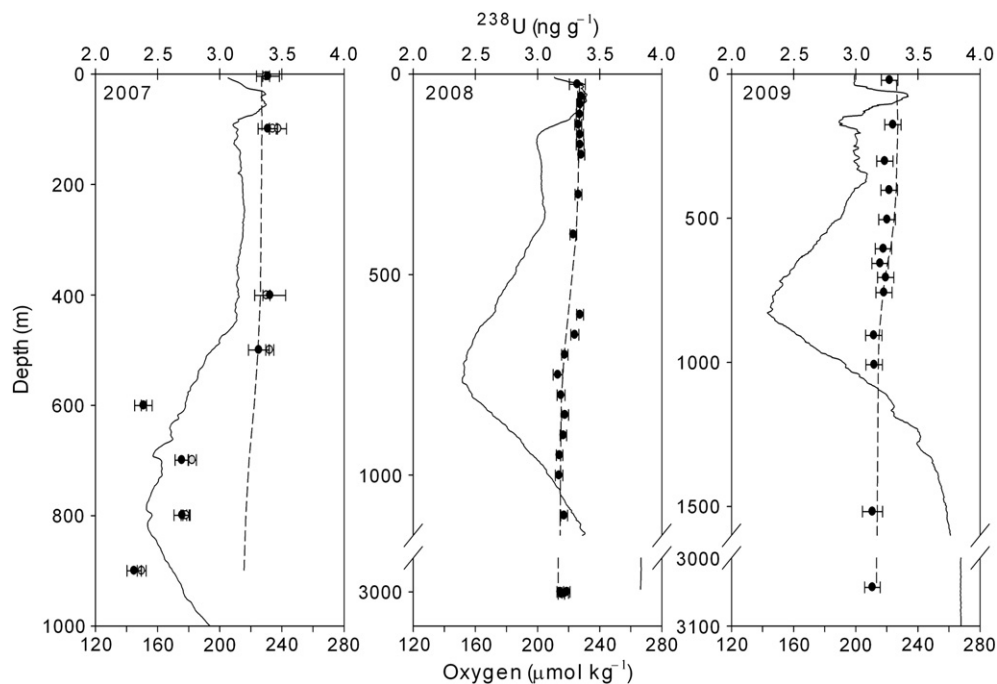
Fig. 2. Measured ^{238}U as a function of depth during three occupations of the Bermuda Atlantic Time-series Study site. Subsamples of the 2007 samples were prepared and measured by ICP-MS at least twice, some three times, and are denoted by white, gray, and black symbols. The dashed line is the ^{238}U concentration estimated from salinity using the regression produced in this study. Dissolved oxygen (solid line) from the CTD is also shown.

(Kochenov et al., 1977; Mohogheghi and Goldhaber, 1982). Thus it is not likely that conditions immediately prior to or during our occupation of the BATS site in June 2007 were conducive to U(VI) reduction and removal.

The third hypothesis, that we consider most likely, is that uranium was removed from the water prior to its arrival at the BATS site and the resulting signal was maintained during advection. One mechanism for removal of uranium from the water column is the accumulation of uranium in suboxic and anoxic sediments (Dunk et al., 2002; Morford and Emerson, 1999). This accumulation arises when uranium reduction from porewaters to the sediment occurs close to the sediment-water interface, which creates a concentration gradient in the porewater leading to a diffusive flux of uranium from seawater and into the sediments. Uranium accumulation rates are an order of magnitude higher in anoxic sediments compared to suboxic continental shelf and slope sediments. However, the greater spatial coverage of shelf and slope sediments makes these anoxic sediments an equally significant sink of uranium from the ocean (Barnes and Cochran, 1990; Dunk et al., 2002; Klinkhammer and Palmer, 1991).

A second mechanism for uranium removal is the co-precipitation of uranium with iron hydroxide particles. Co-precipitation of uranium with iron hydroxide particles has been documented in the laboratory with solutions of iron and uranium and particulate material from a seasonally anoxic lake and also in hydrothermal vent plumes (Bruno et al., 1995; Edmonds and German, 2004; Liger et al., 1999). Over the continental shelf, a similar co-precipitation process could occur when Fe (II) is remobilized from the sediments and precipitates as iron hydroxide particles (Johnson et al., 1999). These shelf-derived iron particles could then passively sink out of the water column as they are transported from their source to the ocean interior (Lam et al., 2006). To demonstrate the potential of the removal mechanisms proposed in this third hypothesis, a careful study of these redox-sensitive, ocean-margin processes would be needed.

The third hypothesis requires both uranium removal and lateral transport. The importance of lateral transport to the BATS region has

been shown in studies of other geochemical tracers. For example, recent work that investigated the source of trace metal fluxes in sediment traps between 500 and 1500 m near the BATS site, suggested that lateral advection from the continental shelf/slope was a significant source of material (Huang and Conte, 2009). Another study suggested that sediments on the Bermuda rise appeared to have been influenced by advection of material from the Nova Scotia margin based on the presence of anomalously old, but recently deposited, haptophyte-derived alkenones (Ohkouchi et al., 2002).

Anomalies in the ^{234}U/^{238}U ratios of the 2007 samples may have provided evidence for previous contact of the water with sediments on the ocean margin. Unfortunately, there was not enough sample volume remaining to measure ^{234}U/^{238}U. In revisiting the site in 2008 and 2009, we hoped to recapture this anomalous feature but as shown in Fig. 2, no such feature was observed and without other tracers, its source remains elusive.

The impetus for this study was the observation of unique deficit (^{234}Th$<$^{238}U) features below 500 m in ^{234}Th profiles taken during the EDDIES study near the BATS site in 2005 (Fig. 3, left panel). Typically, ^{234}Th deficits are constrained to the depths of photosynthetic particle formation and export. There have been only a few reported instances of similar deficit features at depth (Benitez-Nelson et al., 2001a; Coppola et al., 2005; Schmidt, 2006). The best resolved example in the open ocean is from the subtropical Pacific in the winter of 1999/2000 (Benitez-Nelson et al., 2001a). The origin of the intermediate water deficit in ^{234}Th was attributed to particle transformations at depth such as fecal pellet production by zooplankton or aggregation by salps and appendicularians.

The ^{234}Th profiles collected during the EDDIES study that displayed a ^{234}Th deficit at depth (Fig. 3, left panel) were all taken from the core of an anticyclonic mode-water eddy. The nutrient and oxygen concentrations at these depths in the eddy were unlike the local, surrounding conditions near the BATS site and together with temperature and salinity anomalies suggest that they were part of a coherent water mass that was held within the eddy and transported laterally from another location (Li and Hansell, 2008; McGillicuddy Jr.
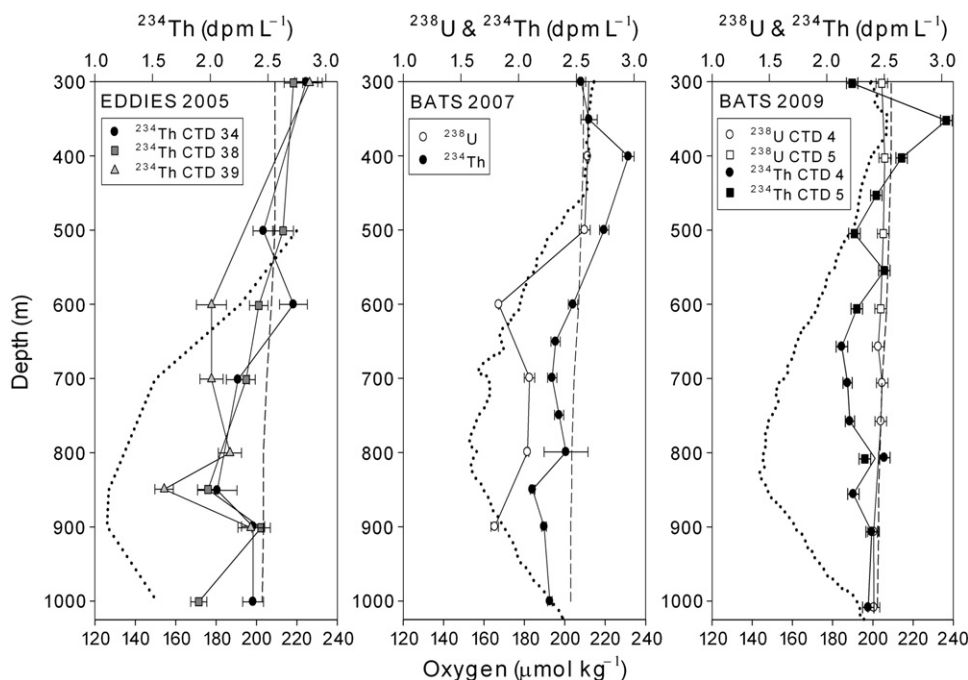
Fig. 3. ^{234}Th profiles from three occupations of the BATS site. ^{238}U derived from salinity (dashed line) and O$_2$ concentrations (dotted line) are shown in all panels. Note that only the 300 to 1000 m section of these profiles are shown. a) Three ^{234}Th profiles collected during the EDDIES study (solid lines) that have deficit features at depth. b) Salinity-derived ^{238}U (dashed line) compared to measured ^{238}U during June 2007 at the BATS site. The ^{234}Th profile was collected simultaneously and shows evidence of non-equilibrium behavior at depth. c) A ^{234}Th/^{238}U profile from the BATS site in September 2009 made up of samples from two casts — CTD 4 (circles) and 5 (squares). ^{238}U (white) is conservative with salinity while ^{234}Th (black) demonstrates non-equilibrium behavior at depth.

et al., 2007). The unique biogeochemical parameters including elevated chlorophyll and low oxygen at depth were constrained to the eddy center, which was estimated, to be on the order of only 10 km (McGillicuddy Jr. et al., 2007). With this degree of small-scale patchiness, it is not surprising that these profiles of ^{234}Th with deficits at depth are a rare observance.

In 2007, repeat measurements of ^{234}Th were made at the BATS site but, as described above, an anomaly in ^{238}U concentration between 600 and 1000 m was observed (Fig. 3, middle panel). What appeared to be a deficit in ^{234}Th in 2007 is in fact an excess of ^{234}Th at depth. One factor that could complicate the interpretation of this ^{234}Th profile is that if and when ^{238}U was removed to the sediments, ^{234}Th may also have been removed. However, if the transit time of the water mass from the margin to the BATS site was on the time-scale of 3–6 months, most of the ^{234}Th would have grown back in to secular equilibrium with ^{238}U. In 2009, no anomalies in ^{238}U concentration were observed yet there was again a deficit of ^{234}Th between 500 and 900 m indicating a more local, or at least a more recent, scavenging process had taken place in deep waters (Fig. 3, right panel). All ^{234}Th measurements have been corrected for low sample recoveries and all measurement uncertainty has been propagated throughout the derivation of ^{234}Th activity so we do not have reason to believe that this is an analytical error. The ^{234}Th deficit appears to be a real feature of the profile. One hypothesis for the formation of a ^{234}Th deficit at depth is the accumulation of small, slowly sinking particles on density gradients that aggregate into larger, fast-sinking particles (MacIntyre et al., 1995). We do not believe that this is occurring in the mid-water column (500–1000 m) at BATS because of the lack of a significant density gradient at these depths. A more likely hypothesis for the formation of a ^{234}Th deficit at depth is that filter feeders such as salps are consuming and repackaging small, slow sinking particles into large, very fast sinking fecal pellets (Sutherland et al., 2010). While we cannot currently identify the exact source of these ^{234}Th deficits in the mesopelagic, we believe that they warrant further study as potential aggregation or repackaging processes could have an important role in the transfer of carbon to the deep ocean.

5. Conclusion

In this work we present a new relationship between salinity and ^{238}U in the open ocean based on a large number of measurements from a single laboratory measured using sensitive isotope dilution mass spectrometry techniques. IAPSO Standard Seawater was used as an internal laboratory standard to establish the reproducibility of our purification and analytical methods. Also, our spike is well calibrated based on a gravimetric standard and years of replicate measurements for equilibrium rock standards.

For a sample with a salinity of 35, the percent difference between using the Chen et al. (1986) relationship versus using the relationship established here is 1.3% although the values agree within error. However, the relationship derived from this data set spans a salinity range twice as large as the Chen et al. data set and is based on 87 sample measurements versus 21. We therefore recommend the use of the following equations with 1σ uncertainty for estimation of ^{238}U from salinity:

$$\left(\text{ng g}^{-1}\right): {}^{238}\text{U}(\pm 0.061) = 0.100 \times S - 0.326 \tag{4}$$

$$\left(\text{dpm L}^{-1}\right): {}^{238}\text{U}(\pm 0.047) = 0.0786 \times S - 0.315. \tag{5}$$

While most measurements of ^{238}U were conservative with salinity, a few samples from the Southern Ocean exhibited a small positive deviation from this behavior. Another example of departure from conservative behavior was the negative deviation of ^{238}U from salinity between 500 and 1000 m at the BATS site in 2007. We hypothesize that this feature was neither the result of analytical bias of our measurements nor a local removal event, but rather the advected signal of a remote removal process associated with reducing sediments common at ocean margins. In addition, our observations of ^{234}Th deficits in the mesopelagic hint at processes previously unexplored with this isotope system. We encourage other ^{234}Th studies to expand their sampling efforts into the depths of the

mesopelagic zone in the hope of gaining a greater understanding of particle cycling and export. Our observation of a ^{238}U anomaly at these depths in 2007 however should be a caveat for future studies. We recommend collecting small, archive seawater samples in conjunction with all ^{234}Th samples that may be analyzed for ^{238}U at a later date should the ^{234}Th data suggest that such an anomalous ^{238}U feature may be present.

Acknowledgments

References

Andersen, M.B., et al., 2007. The tracing of riverine U in Arctic seawater with very precise U-234/U-238 measurements. Earth and Planetary Science Letters 259, 171–185.

Anderson, R.F., Fleisher, M.Q., LeHuray, A.P., 1989. Concentration, oxidation state, and particulate flux of uranium in the Black Sea. Geochimica et Cosmochimica Acta 53, 2215–2224.

Bacon, M.P., Cochran, J.K., Hirschberg, D., Hammar, T.R., Fleer, A.P., 1996. Export flux of carbon at the equator during the EqPac time-series cruises estimated from ^{234}Th measurements. Deep-Sea Research II 43 (4–6), 1133–1153.

Barnes, C.E., Cochran, J.K., 1990. Uranium removal in oceanic sediments and the oceanic U balance. Earth and Planetary Science Letters 97, 94–101.

Benitez-Nelson, C., Buesseler, K.O., Karl, D.M., Andrews, J., 2001a. A time-series study of particulate matter export in the North Pacific Subtropical Gyre based on Th-234: U-238 disequilibrium. Deep-Sea Research I 48 (12), 2595–2611.

Benitez-Nelson, C.R., et al., 2001b. Testing a new small-volume technique for determining ^{234}Th in seawater. Journal of Radioanalytical and Nuclear Chemistry 248 (3), 795–799.

Bhat, S.G., Krishnaswamy, S., Lal, D., Rama, Moore, W.S., 1969. ^{234}Th/^{238}U ratios in the ocean. Earth and Planetary Science Letters 5, 483–491.

Bruno, J., De Pablo, J., Duro, L., Figuerola, E., 1995. Experimental study and modeling of the U(VI)-Fe(OH)3 surface precipitation/coprecipitation equilibria. Geochimica et Cosmochimica Acta 59 (20), 4113–4123.

Buesseler, K.O., Bacon, M.P., Cochran, J.K., Livingston, H.D., 1992. Carbon and nitrogen export during the JGOFS North Atlantic Bloom Experiment estimated from ^{234}Th:^{238}U disequilibria. Deep-Sea Research I 39 (7–8), 1115–1137.

Buesseler, K.O., et al., 2001. An intercomparison of small- and large-volume techniques for thorium-234 in seawater. Marine Chemistry 74 (1), 15–28.

Buesseler, K.O., et al., 2008a. Particle fluxes associated with mesoscale eddies in the Sargasso Sea. Deep-Sea Research II 55 (10–13), 1426–1444.

Buesseler, K.O., et al., 2008b. Thorium-234 as a tracer of spatial, temporal and vertical variability in particle flux in the North Pacific. Deep-Sea Research Part I-Oceanographic Research Papers 56 (7), 1143–1167.

Carroll, J., Moore, W.S., 1994. Uranium removal during low discharge in the Ganges-Brahmaputra mixing zone. Geochimica et Cosmochimica Acta 58, 4987–4995.

Chen, J.H., Wasserburg, G.J., 1981. Isotopic determination of uranium in picomole and subpicomole quantities. Analytical Chemistry 53, 2060–2067.

Chen, J.H., Edwards, R.L., Wasserburg, G.J., 1986. ^{238}U, ^{234}U and ^{232}Th in seawater. Earth and Planetary Science Letters 80 (3–4), 241–251.

Cochran, J.K., 1992. The oceanic chemistry of the U- and Th- series nuclides. Book Section: Uranium Series Disequilibrium: Application to Environmental Problems. .

Coppola, L., Roy-Barman, M., Mulsow, S., Povinec, P., Jeandel, C., 2005. Low particulate organic carbon export in the frontal zone of the Southern Ocean (Indian sector) revealed by ^{234}Th. Deep-Sea Research I 52 (1), 51–68.

Delanghe, D., Bard, E., Hamelin, B., 2002. New TIMS constraints on the uranium-238 and uranium-234 in seawaters from the main ocean basins and the Mediterranean Sea. Marine Chemistry 80 (1), 79–93.

Djogić, R., Sipos, L., Branica, M., 1986. Characterization of uranium (VI) in seawater. Limnology and Oceanography 31 (5), 1122–1131.

Dunk, R.M., Mills, R.A., Jenkins, W.J., 2002. A reevaluation of the oceanic uranium budget for the Holocene. Chemical Geology 190 (1–4), 45–67.

Edmonds, H.N., German, C.R., 2004. Particle geochemistry in the Rainbow hydrothermal plume, Mid-Atlantic Ridge. Geochimica et Cosmochimica Acta 68 (4), 759–772.

Feng, H., Cochran, J.K., Hirschberg, D.J., 2002. Transport and sources of metal contaminants over the course of tidal cycle in the turbidity maximum zone of the Hudson River estuary. Water Research 36 (3), 733–743.

Gustafsson, O., Buesseler, K.O., Geyer, W., Rockwell, Moran, Bradley, S., Gschwend, P.M., 1998. On the relative significance of horizontal and vertical transport of chemicals in the coastal ocean: application of a two-dimensional Th-234 cycling model. Continental Shelf Research 18, 805–829.

Huang, S., Conte, M.H., 2009. Source/process apportionment of major and trace elements in sinking particles in the Sargasso Sea. Geochimica et Cosmochimica Acta 73, 65–90.

Jaffey, A.H., Flynn, K.F., Glendenin, L.E., Bentley, W.C., Essling, A.M., 1971. Precision measurement of half-lives and specific activities of U-235 and U-238. Physical Review C 4 (5), 1889–1906.

Johnson, K.S., Chavez, F.P., Friederich, G.E., 1999. Continental-shelf sediment as a primary source of iron for coastal phytoplankton. Nature 398, 697–700.

Klinkhammer, G.P., Palmer, M.R., 1991. Uranium in the oceans — where it goes and why. Geochimica et Cosmochimica Acta 55, 1799–1806.

Kochenov, A., Korolev, K.G., Dubinchuk, V.T., Medvedev Yu, L., 1977. Experimental data on the conditions of precipitation of uranium from acqueous solutions. Geochemistry International 14, 82–87.

Ku, T.L., Knauss, K.G., Mathieu, G.G., 1977. Uranium in open ocean: concentration and isotopic composition. Deep-Sea Research 24 (11), 1005–1017.

Lam, P.J., et al., 2006. Wintertime phytoplankton bloom in the subarctic Pacific supported by continental margin iron. Global Biogeochemical Cycles, 20.

Li, Q.P., Hansell, D.A., 2008. Nutrient distributions in baroclinic eddies of the oligotrophic North Atlantic and inferred impacts on biology. Deep-Sea Research II 55, 1291–1299.

Liger, E., Charlet, L., Van Cappellen, P.V., 1999. Surface catalysis of uranium(VI) reduction by iron(II). Geochimica et Cosmochimica Acta 63 (19/20), 2939–2955.

MacIntyre, S., Alldredge, A.L., Gotschalk, C.C., 1995. Accumulation of marine snow at density discontinuities in the water column. Limnology and Oceanography 40 (3), 449–468.

McGillicuddy Jr., D.J., et al., 2007. Eddy-wind interactions stimulate extraordinary mid-ocean plankton blooms. Science 316, 1021–1026.

McKee, B.A., DeMaster, D.J., Nittrouer, C.A., 1987. Uranium geochemistry on the Amazon shelf: evidence for uranium release from bottom sediments. Geochimica et Cosmochimica Acta 51, 2779–2786.

Millero, F.J., Poisson, A., 1981. International one-atmosphere equation of state of seawater. Deep-Sea Research I 28A (6), 625–629.

Mohogheghi, A., Goldhaber, M., 1982. Kinetics of uranyl ion reduction by acqueous sulfide at 35°C (abstr.). Geological Society of America 568.

Morford, J.L., Emerson, S., 1999. The geochemistry of redox sensitive trace metals in sediments. Geochimica et Cosmochimica Acta 63, 1735–1750.

Ohkouchi, N., Eglinton, T.I., Keigwin, L.D., Hayes, J.M., 2002. Spatial and temporal offsets between proxy records in a sediment drift. Science 298, 1224–1227.

Osmond, J.K., Cowart, J.B., 1992. Ground water. Uranium-Series Disequilibrium: Applications to Earth, Marine and Environmental Sciences. Clarendon Press, Oxford.

Pates, J.M., Muir, G.K.P., 2007. U-salinity relationships in the Mediterranean: implications for Th-234/U-238 particle flux studies. Marine Chemistry 106, 530–545.

Pike, S.M., Buesseler, K.O., Andrews, J., Savoye, N., 2005. Quantification of ^{234}Th recovery in small volume sea water samples by inductively coupled plasma mass spectrometry. Journal of Radioanalytical and Nuclear Chemistry 263 (2), 355–360.

Rengarajan, R., Sarin, M.M., Krishnaswami, S., 2003. Uranium in the Arabian Sea: role of denitrification in controlling its distribution. Oceanologica Acta 26 (5–6), 687–693.

Robinson, L.F., Belshaw, N.S., Henderson, G.M., 2004. U and Th concentrations and isotope ratios in modern carbonates and waters from the Bahamas. Geochimica et Cosmochimica Acta 68 (8), 1777–1789.

Rodriguez y Baena, A.M., et al., 2008. Th-234-based carbon export during an ice-edge bloom: sea-ice algae as a likely bias in data interpretation. Earth and Planetary Science Letters 269, 595–603.

Rutgers van der Loeff, M., et al., 2006. A review of present techniques and methodological advances in analyzing ^{234}Th in aquatic systems. Marine Chemistry 100 (3–4), 190–212.

Santschi, P.H., et al., 2006. Thorium speciation in seawater. Marine Chemistry 100, 250–268.

Schmidt, S., 2006. Impact of the Mediterranean Outflow Water on the particle dynamics in intermediate waters of the Northeast Atlantic as revealed by Th-234 and Th-228. Marine Chemistry 100, 289–298.

Schmidt, S., Reyss, J.L., 1991. Uranium concentrations of Mediterranean seawaters with high salinities. Comptes Rendus de l'Academie des Sciences Serie II 312 (5), 479–484.

Sims, K.W.W., et al., 2008. An inter-laboratory assessment of the thorium isotopic composition of synthetic and rock reference materials. Geostandards and Geoanalytical Research 32 (1), 65–91.

Sutherland, K.R., Madin, L.P., Stocker, R., 2010. Filtration of submicrometer particles by pelagic tunicates. Proceedings of the National Academy of Sciences 107 (34), 15129–15134.

UNESCO, 1983. Algorithms for computation of fundamental properties of seawater. UNESCO Technical Papers in Marine Science, 44.

Zheng, J., Yamada, M., Aono, T., Kusakabe, M., 2006. Vertical distribution of uranium concentrations and U-238/U-238 atom ratios in the coastal water off Aomori, Japan: a survey prior to the operation of a nuclear fuel reprocessing facility. Journal of Radioanalytical and Nuclear Chemistry 270 (3), 669–675.